EXPERIMENTAL DEMONSTRATION OF REAL TIME GRADIENT GAIN CORRECTION FOR SODIUM BEACON LASER GUIDE STAR: POSTPRINT

Katia Shtyrkova, et al.

Air Force Research Laboratory
3500 Aberdeen Ave SE
Kirtland AFB, NM 87117

01 June 2010

Technical Paper

AIR FORCE RESEARCH LABORATORY
Directed Energy Directorate
3550 Aberdeen Ave SE
AIR FORCE MATERIEL COMMAND
KIRTLAND AIR FORCE BASE, NM 87117-5776

REPORT DOCUMENTATION PAGE

Public reporting burden for this collection of information is estimated to average 1 hour per response, including the time for reviewing instructions, searching existing data sources, gathering and maintaining the data needed, and completing and reviewing this collection of information. Send comments regarding this burden estimate or any other aspect of this collection of information, including suggestions for reducing this burden to Department of Defense, Washington Headquarters Services, Directorate for Information Operations and Reports (0704-0188), 1215 Jefferson Davis Highway, Suite 1204, Arlington, VA 22202-4302. Respondents should be aware that notwithstanding any other provision of law, no person shall be subject to any penalty for failing to comply with a collection of information if it does not display a currently valid OMB control number. **PLEASE DO NOT RETURN YOUR FORM TO THE ABOVE ADDRESS.**

1. REPORT DATE *(DD-MM-YYYY)* 01-06-2010	2. REPORT TYPE Technical Paper	3. DATES COVERED *(From - To)* Oct 1, 2008- Jun 1, 2010
4. TITLE AND SUBTITLE Experimental Demonstration of Real Time Gradient Gain Correction for Sodium Beacon Laser Guide Star: Postprint		**5a. CONTRACT NUMBER** In House DF702151
		5b. GRANT NUMBER
		5c. PROGRAM ELEMENT NUMBER 62890F
6. AUTHOR(S) Katia Shtyrkoa, *Michael D. Oliker, Kevin P. Vitayaudom, *Denis W. Oesch, Darryl J. Sanchez, Patrick R. Kelly, Catylon M. Tewksbury-Christle, Julie C. Smith		**5d. PROJECT NUMBER** 2301
		5e. TASK NUMBER SJ
		5f. WORK UNIT NUMBER 41
7. PERFORMING ORGANIZATION NAME(S) AND ADDRESS(ES) Air Force Research Laboratory *Science Applications International 3550 Aberdeen Ave SE 6109 Airpark Rd Southeast Kirtland AFB, NM 87117 Albuquerque, NM 87106		**8. PERFORMING ORGANIZATION REPORT NUMBER**
9. SPONSORING / MONITORING AGENCY NAME(S) AND ADDRESS(ES) Air Force Research Laboratory 3550 Aberdeen Ave Kirtland AFB, NM 87117		**10. SPONSOR/MONITOR'S ACRONYM(S)** AFRL/RDS
		11. SPONSOR/MONITOR'S REPORT NUMBER(S) AFRL-RD-PS-TP-2010-1024

12. DISTRIBUTION / AVAILABILITY STATEMENT

Approved for Public Release

13. SUPPLEMENTARY NOTES
377ABW-2010-1195, July 29, 2010. "GOVERNMENT PURPOSE RIGHTS"

14. ABSTRACT

One of the problems associated with the use of the sodium laser guide star as a beacon for an adaptive optics system is the changes in the sensitivity of the wavefront sensor caused by the extended nature of the sodium layer. Shack-Hartmann wavefront sensors use quad cell detectors to estimate the amount of x- and y- gradients in each sub-aperture. The gradients are multiplied by a constant gain factor that is equal in the x and y directions. Due to the non-zero thickness of the sodium layer, the wavefront sensor sees elongated, rather than round, spot, which causes different gains in the x- and y- directions. This directly impacts the reconstructed phase and thus degrades the closed loop AO performance. This paper presents an experimental demonstration of the null space technique that allows for real time extended spot gain correction in a closed loop AO operation. The implementation of the technique in the ASALT laboratory testbed is described, system performance degradation for incorrect gains is measured, and null space corrected performance for different atmospheres is presented.

15. SUBJECT TERMS

16. SECURITY CLASSIFICATION OF:			17. LIMITATION OF ABSTRACT	18. NUMBER OF PAGES	19a. NAME OF RESPONSIBLE PERSON Patrick Kelly
a. REPORT Unclassified	**b. ABSTRACT** Unclassified	**c. THIS PAGE** Unclassified	SAR	20	**19b. TELEPHONE NUMBER** *(include area code)* 505-846-2094

This page is intentionally left blank.

Experimental Demonstration Of Real Time Gradient Gain Correction For Sodium Beacon Laser Guide Star

Katia Shtyrkova[1]*, Michael D. Oliker[2], Kevin P. Vitayaudom[1],
Denis W. Oesch[2], Darryl J. Sanchez[1], Patrick R. Kelly[1], Carolyn
M. Tewksbury-Christle[1], Julie C. Smith[1]

[1]*Starfire Optical Range, AFRL/RDS, Kirtland AFB, Albuquerque, NM. 87117, USA*

[2]*Science Applications International Corporation, Albuquerque, New Mexico, USA*

*Corresponding author: katia.shtyrkova@kirtland.af.mil

Abstract: One of the problems associated with the use of the sodium laser guide star as a beacon for an adaptive optics system is the changes in the sensitivity of the wavefront sensor caused by the extended nature of the sodium layer. Shack-Hartmann wavefront sensors use quad cell detectors to estimate the amount of x- and y- gradients in each sub-aperture. The gradients are multiplied by a constant gain factor that is equal in the x and y directions. Due to the non-zero thickness of the sodium layer, the wavefront sensor sees an elongated, rather than round, spot, which causes different gains in the x- and y-directions. This directly impacts the reconstructed phase and thus degrades the closed loop AO performance. This paper presents an experimental demonstration of the null space technique that allows for real time extended spot gain correction in a closed loop AO operation. The implementation of the technique in the ASALT laboratory testbed is described, system performance degradation for incorrect gains is measured, and null space corrected performance for different atmospheres is presented.

Keywords: adaptive optics, wavefront sensor, laser guidestar, sodium beacon, perspective elongation

1. Nomenclature

- AO - Adaptive Optics

- AFRL - Air Force Research Laboratory

- ASALT - Atmospheric Simulation and Adaptive Optics Laboratory Team

- ACS - Atmospheric Compensation Simulator (software package)

- ATS - Atmospheric Turbulence Simulator (hardware on the table)

- DM - Deformable Mirror

- LGS - Laser Guide Star

- NGAS - Sodium Guidestar Adaptive Optics for Space Situational Awareness

- NUGE - Non-Uniform Gain Experiment

- RTR - Real Time Reconstructor

- SH - Shack Hartmann

- SM - Steering Mirror

- SRI - Self Referencing Interferometer

- WFS - Wavefront Sensor

2. Introduction

The Air Force Research Laboratory's Starfire Optical Range uses a sodium laser guide star as a beacon for its 3.5 m telescope AO system. Sodium laser guide stars have been used for the purpose of beacons in adaptive optics since 1997 [1]. While they provide significantly improved closed loop performance over Rayleigh beacons, they also pose numerous problems. Some of those problems are associated with the sodium layer, such as its varying thickness, changing density of the scatterers (column abundance), and extended nature of the formed beacon. This paper focuses on the extended nature of the beacon and its effects on the LGS WFS response, which leads to the degradation of the reconstructed phase, and consequently decreased Strehl ratio.

The mesospheric sodium layer is located at about 90 km above the sea level, and has a thickness that varies from 8 to 16 km [2]. Due to this considerable thickness, a LGS created in this layer by a laser beam tuned to the sodium D_2 line at 589 nm, appears as an

extended source (see Figure 1). The extended nature of the source presents two potential problems for WFS. First, the spots will appear extended on the WFS camera. Second, the spots will look different from sub-aperture to sub-aperture, and thus the WFS gains in each sub-aperture will differ from one another.

Numerous models have been proposed by the astronomical community that estimate the effects of both the extended nature of the beacon and the per-sub-aperture gain variations [3], [4], [5]. Most common techniques include the per-sub-aperture specific gains applications [6], noise-optimal matched filter spot position estimation algorithm [7], [8], dynamic refocusing of the telescope [9], and dynamically steered SH sub-apertures [10].

In this paper we present a perspective elongation solution, based on the slope discrepancy space of the reconstructor matrix. Perspective elongation is assumed to vary only in the x- and y- directions of the primary aperture, and not on the sub-aperture basis. The null space of the reconstructor is used in order to separate extended beacon effects from the atmospheric turbulence, reference projection into the null space is compared with the frame-by-frame gradients, and correction factor is calculated and applied to gradients in real time.

3.   Effects of the Extended Source

Figure 1 shows the geometry of the sodium layer with relation to the primary imaging telescope, and the sodium beacon launching telescope. Distance between the launching and imaging telescopes, thickness of the sodium layer, and the zenith angle are the primary variables responsible for the extended nature of the sodium LGS.
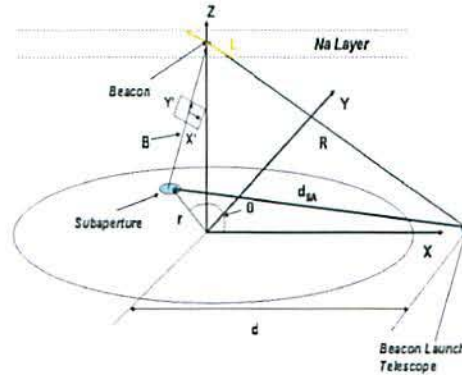

Fig. 1. *Geometry of the sodium layer, Na guide star, and the telescope.*

In astronomical AO systems, Shack-Hartmann WFSs are most commonly used for sensing the wavefront of LGS. The sensor consists of a lenslet array, where each lens (each sub-aperture) is followed by a quad cell detector (2×2 array of active pixels), or higher resolution detector, which is typically binned down to a 2×2 quad cell. A typical quad cell with a focused spot on it is shown in Figure 2. The gradients for such a sub-aperture are calculated using formulas 1 and 2, where a, b, c, and d are light intensities measured by corresponding pixels, and subsequently multiplied by a calibration factor, which takes into account local measured biases.

$$xgrads = \frac{(b+d) - (a+c)}{a+b+c+d} \tag{1}$$

$$ygrads = \frac{(a+b) - (c+d)}{a+b+c+d} \tag{2}$$

Sensitivity of the WFS for a particular spot size can be determined by scanning the spot across the quad cell, and plotting calculated gradients versus the spot centroid. The resulting plot is called a transfer curve (or, sometimes, the S- curve), where the slope in the middle is the sensitivity of the WFS, and the inverse of the slope is the gain. For a round spot, x- and y- gains are equal (see Figure 2). Larger spots produce less steep curves, the sensitivity goes down, and the gains of the WFS go up, as is illustrated in Figure 3. When the object being imaged is extended, the quad cell has different x- and y- responses, which results in the transfer curves, and subsequently sensitivities and gains being different in the x- and y- directions. Figure 4 shows a simulated oblong spot along with corresponding x- and y- transfer curves.
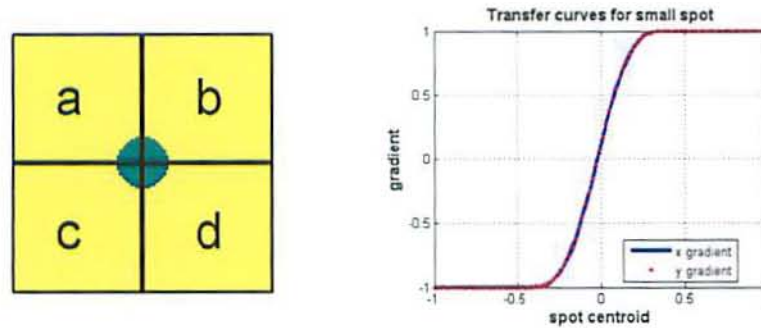

Fig. 2. *Small round spot at the center of the quad cell produces identical x- and y- transfer curves, and thus equal x- and y- gains.*
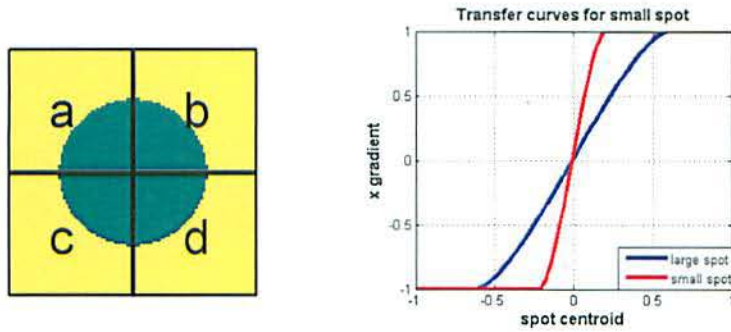
Fig. 3. *Large round spot produces equal transfer curves in x- and y- direction, but the transfer curves are different from the small spot curves. In particular, the slope in the middle is less for larger spot, resulting in greater required WFS gains.*
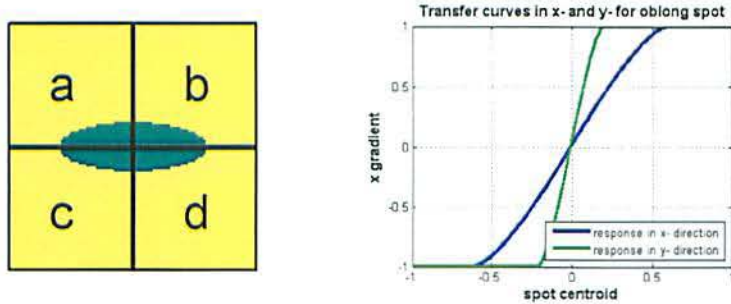

Fig. 4. *Oblong spot produces different quad cell responses in x- and y-directions. This results in different transfer curves with different slopes. The x- and y- WFS gains are different.*

Figure 5 shows ACS software simulation data for a high resolution SH camera for sodium beacon LGS with mild turbulence. The apparent extension of the spot varies from sub-aperture to sub-aperture, though only one sub-aperture is shown. Produced transfer curves for x- and y- directions are shown on the right in Figure 5. It is important to point out that, even though the curves look almost identical, the change in sensitivity, and thus the change in gains between the x- and y- directions is significant. Data calculated directly from Figure 5 is shown in Table 1, where the change in going from x- to y- gains is 14.54%. This is significant and will noticeably degrade the Strehl ratio of the closed loop performance. The problem that this paper addresses is dynamically changing gains of the WFS, which are caused by the extended nature of sodium beacon, and are uncorrected in normal closed loop AO runs.
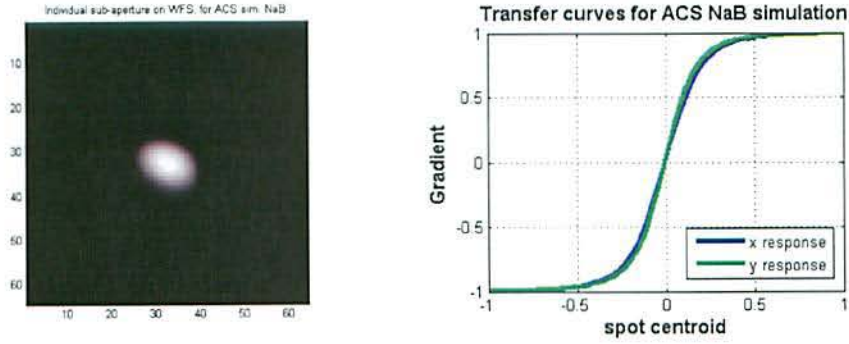
Fig. 5. *ACS simulated sodium beacon spot, one sub-aperture, with mild turbulence.*

	Sodium Beacon, 1 sub-aperture
X sensitivity	0.6781
Y sensitivity	0.7935
X gain	1.4748
Y gain	1.2603

Table 1. Sensitivities and gains in x- and y- for NaB ACS simulated spots, one sub-aperture.

4. Theoretical Solution - The Null Space of the Reconstructor

The solution to perspective elongation presented in this paper identifies system degradations due to the atmosphere and elongated sources separately. AFRL developed the Nullspace algorithm for gain correction, which uses the null space of the reconstructor to look for gradient bleed through. The null space (slope discrepancy space) of the reconstruction matrix contains very little reconstructible atmospheric energy (almost none), however it does see the gradient components. By projecting the reference gradient components into the null space, and comparing them with frame-by-frame gradient projections, we calculate the so-called gradient "bleed through", which shows the effects of the extended beacon on the frame-by-frame gradients.

4.1. Null Space of the Reconstructor

To explain the concept of null space in more detail, we start with the G matrix, which is used to map the phase into gradients. Figure 6 (left) shows the G matrix decomposed into three separate matrices by singular value decomposition method: $G = U \cdot S \cdot V^T$. The V

matrix consists of the orthogonal unit vectors that span the space of active mirror actuators. The U matrix consists of orthogonal unit vectors that span the space of all possible gradients. Note that the number of active gradients is greater than the number of actuators by about a factor of two, which means the system is overdetermined. The S matrix takes the amount of one mode in V and scales it to the corresponding element of U. By taking the pseudo-inverse of G, the RTR matrix is obtained, which takes in the gradients and reconstructs the phase. The RTR matrix can be expressed similarly in terms of U, S, and V matrices: $RTR = V \cdot S_{inv} \cdot U^T$ - see Figure 6 (right). The rows of the U^T matrix span the space of all possible gradients (it creates the gradient "modes"). By multiplying U^T by the vector of frame-by-frame gradients, we get the amount of gradients in each of the possible gradient modes. S_{inv} matrix converts possible gradients to mirror actuators. However, only the first $M \times 2N$ gradient modes (where M is the number of active actuators, 2N is the number of possible gradients) are converted into the reconstructed phase, which corresponds to possible reconstructible modes of the reconstructor. The remaining $[2N - M] \times 2N$ modes are multiplied by zero, they are not affected by the atmospheric energy and are not manifested in the resulting reconstructed phase. Those modes span the null space. Note that the null space model was originally developed for NGAS program, and the dimensions of the G, U, S, V and RTR matrices shown in Figure 6 correspond to the system parameters of NGAS. Very little reconstructible atmospheric energy gets into the null space, with the exception of high frequency modes, which cannot be corrected by the DM. By looking at the power spectral density of each mode for reconstructible modes and for null space modes, it is apparent that the null space does not contain much of the reconstructible atmospheric energy. Figure 7 illustrates the concept. For the reconstructible modes (left plot) going from open loop to closed loop (from blue to red curves), the energy at lower frequencies decreases significantly. The energy at higher frequencies is unchanged due to the inability of the closed loop AO to compensate for higher frequency turbulence. By contrast, the power in the null space modes (right plot) remains near identical in open (blue curve) and closed (red curve) loop. This signifies the fact that the DM does not affect the energy in null space, and thus it can be used to sense changes in the system unaffected by the atmosphere.
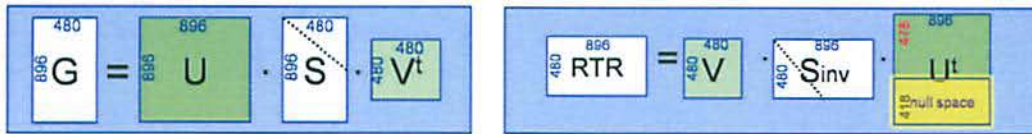

Fig. 6. *G matrix maps the phase into the gradients. Shown is singular value decomposition of the G matrix. RTR matrix is obtained by pseudo-inverting the G matrix. RTR converts gradients into phase.*
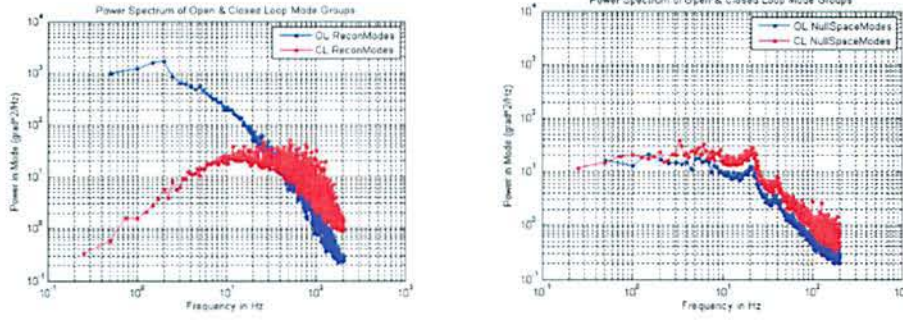
Fig. 7. *Power in the reconstructable modes (left) and null space modes (right) versus frequency for open loop (blue) and closed loop (red).*

4.2. Calculations behind the algorithm

Applying the Nullspace algorithm to closed loop AO data includes two parts - the offline part, which is done once, and the online part, which is calculated on each frame of the new gradients data. For the new reconstructor and/or new reference, the offline part needs to be calculated again. Suppose the number of active X- gradients, equal to the number of active Y- gradients, is N; the number of active actuators is M.

Offline:

- Singular Value Decomposition is used to calculate the null space of the reconstructor, this matrix is called Z ($[2N - M] \times 2N$). Z maps the gradients into the null space.

- Zx and Zy vectors are formed, where Zx is the Z matrix applied to X- gradient components of the reference (reference with Y- components zeroed), and Zy is a vector formed by applying the Z matrix to Y- components of the reference (reference with X- components zeroed). Both Zx and Zy have dimensions of $[2N - M] \times 1$.

- Zx and Zy are combined into one matrix $[2N - M] \times 2$ which is pseudo-inverted to get *Modes2Sensitivity* matrix, with dimensions $2 \times [2N - M]$. This matrix maps the null space spectrum of the averaged gradients into sensitivity values in X- and Y-. It shows how much of the X- and Y- reference is present in the null space.

- *Gradients2Sensitivity* operator is found by multiplying *Modes2Sensitivity* matrix ($2 \times [2N - M]$) by Z matrix ($[2N - M] \times 2N$). The resulting matrix has dimensions of $2 \times 2N$, it maps gradients directly into the sensitivities. In other words, it com-

8

bines the calculation of the null space components of the gradients with that of extracting the sensitivities from those null space components.

Online:

- *Gradients2Sensitivity* operator is used on frame-by-frame gradients to calculate the new sensitivities.

- Gain is calculated as the inverse of the sensitivity: $Gain = 1/Sensitivity$.

- The gains are updated according to the control law:

$$Filtered\_gain(i+1) = A \times leak\_gain(i) + B \times servo\_gain(i). \qquad (3)$$

5. Experimental Setup

5.1. ASALT Lab Optical Bench Layout

The ASALT Laboratory provides a complete bench-top AO system with a capability to simulate a number of atmospheric conditions. The layout of the optical bench used to test the Nullspace algorithm is shown in Figure 8. Note that the system, along with all the atmospheric parameters simulated, is scaled to mimic a 1.5 m telescope system, but could also be scaled to other telescope sizes. A 1550 nm laser is used to simulate the point source (see Section 5.2 for simulation of the extended source) that takes the light through the atmospheric turbulence simulator, which includes two relay telescopes and two phase wheels etched with the Kolmogorov structure function. By exchanging the field lenses and positions of relay telescopes, and by controlling the speed of phase wheel rotations, atmospheric parameters such as Fried's coherence length, Rytov number, and Greenwood frequency can be controlled. Next, the aberrated light beam reflects off the steering mirror, which removes global tip/tilt. The light is then reflected onto off-axis parabolic mirrors, bringing the beam to a collimated space, where the DM applies high order correction to the beam. A Xinetics 941 actuator DM with 31x31 actuators was used for this experiment. After the DM, the light is sent to beamsplitters, which separate the beam into different paths - a SH WFS path, a Scoring Camera path, and a Self-Referencing Interferometer path. The wavefront sensor used for the Nullspace experiment was a 24x24 sub-aperture Shack-Hartmann WFS, with 2x2 active pixel quad cells. A 128x128 pixel scoring camera was used to monitor system performance.
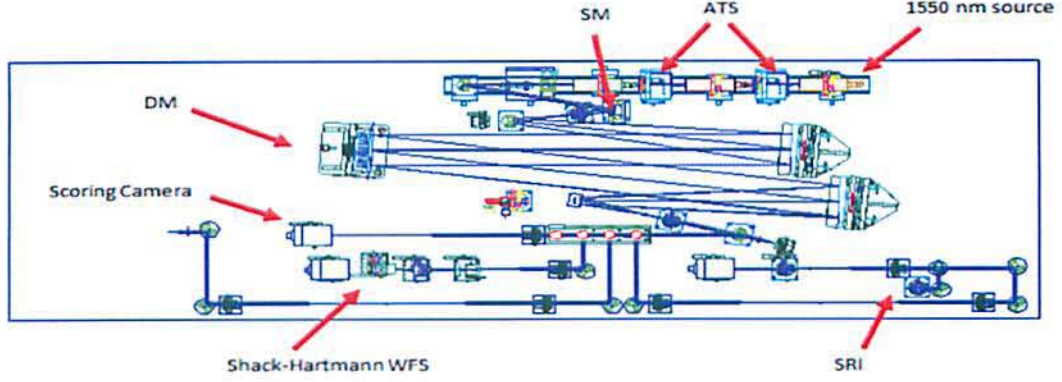
Fig. 8. *ASALT Lab SRI-1 table layout.*

5.2. *Modeling the Extended Source*

While the technique described in this paper focuses on correcting the gains of the WFS due to the extended nature of the source, at the time of this experiment, the ASALT Lab did not have the extended optical source to accurately mimic the sodium beacon. In order to simulate the extended source, the gains of the WFS were intentionally degraded through data post-processing. Gain error was introduced by multiplying closed loop no turbulence (vacuum propagation) gradient gains by a constant factor prior to closing the loop. Two incorrect gain factors were used: kx for x gradients, and ky for y gradients. The gradients were multiplied as follows:

$$x\_gradients = kx \times x\_gradients \qquad (4)$$

$$y\_gradients = ky \times y\_gradients \qquad (5)$$

Figure 9 shows the perfect spot for closed loop AO run on the left, and the spot created by setting kx=0.4 and ky=0.2 on the right. By varying the magnitude of kx and ky, the elongation of the source can be varied in two different directions. For most of the tests presented in this paper, gain factors were set at kx=0.4, ky=0.2. Such values result in poor closed loop performance when the extended nature of the source is uncorrected. While for the real sodium beacon the performance degradation due to the given thickness of the sodium layer is nowhere near as dramatic, the purpose of this paper is to demonstrate that the Nullspace algorithm works well for the worst possible scenario.
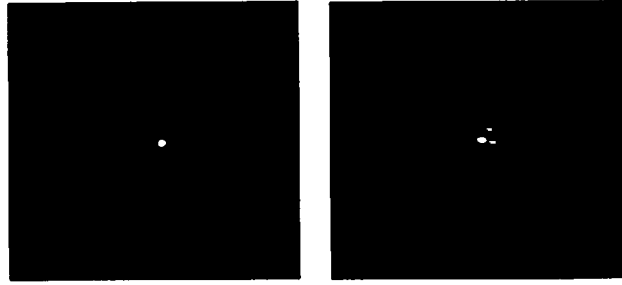
Fig. 9. *Left: Scoring camera image for vacuum case, kx=1.0, ky=1.0. Right: Scoring camera image for vacuum case for kx=0.4, ky=0.2 - intentionally set wrong gains create the elongation of the source.*

5.3. Control System

The ASALT Lab control system uses an interactive environment that combines hardware and software elements, which are run from different computers, as components on the central layout. Figure 10 shows a snap shot of the control layout, which captures one frame (one iteration) of data. Individual components (blocks in Figure 10) are either hardware elements (DM, cameras, tracking controllers, ATS), or software elements, called "processing nodes" that perform specific calculations/data manipulation. Each component has a certain number of inputs, outputs, and so called configuration items, allowing various parameters to be changed dynamically during data runs. Each experiment has its own layout designed for it, with particular components built into it. The flow of data collection is established by connecting all the required components in a specified sequence.
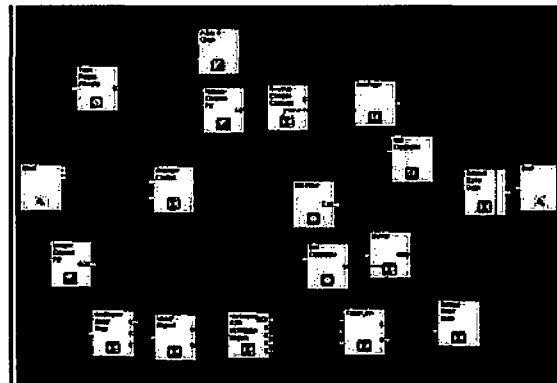

Fig. 10. *Control Console, layout that was used for Nullspace algorithm.*

5.4. Parameter Space

Table 2 shows several sets of atmospheric parameters that were used to test the Nullspace algorithm. Note that for three test runs, a combination of r_0 and Rytov were varied, ranging from severe to mild turbulence. For three other runs, r_0 and Rytov were held constant, but Greenwood frequency was varied. For separate three runs, atmospheric conditions were kept constant, but extended beacon gains kx and ky were changed in order to demonstrate that the algorithm works well with sources of different perspective elongation.

Data Set	Turbulence Set	r_0(cm)	Rytov	f_G(Hz)	kx	ky
1	TR2	7.8	0.25	33.8	0.4	0.2
2	TR1	10.3	0.06	33.8	0.4	0.2
3	TR3	15.32	0.1	33.8	0.4	0.2
4	TR4	15.32	0.1	52.9	0.4	0.2
5	TR5	15.32	0.1	82.6	0.4	0.2
6	TR3	15.32	0.1	33.8	0.4	0.2
7	TR3	15.32	0.1	33.8	1.5	0.5
8	TR3	15.32	0.1	33.8	1.8	1.0

Table 2. Parameter space for testing Nullspace algorithm in ASALT Lab

6. Results and Analysis

Strehl ratio was one of the primary metrics used to analyze the performance of the system under different atmospheric conditions. For this experiment, instantaneous (frame by frame) Strehl was calculated as a 3x3 bucket power around the hottest pixel, normalized by 3x3 bucket power for a vacuum (closed loop no turbulence case). The left plot in Figure 11 shows the instantaneous Strehl ratio, with the blue curve showing the open loop performance, and the pink curve showing the standard closed loop performance under the same atmosphere without any incorrect gains. The black curve was produced with kx=0.4, and ky=0.2, without correcting for those gain errors, which resulted in performance degradation all the way down to open loop level. The green curve shows the data corrected by the Nullspace algorithm, which started at frame 50. It is evident that it took about 25 frames for the Strehl to start going up significantly. At about frame 150 the Nullspace-corrected data starts fluctuating around the regular closed loop AO data. Note that a temporal control law under the Nullspace function sets up how quickly the data is being updated. The right plot in Figure 11 shows the green Nullspace-corrected Strehl data on top, and frame-by-frame kx and ky gradient gains on the bottom (blue and red).

The gains started at kx=0.4, ky=0.2, as was intentionally set up to simulate the extended source, remained constant until frame 50, and started climbing up until they were nearly 1 (correct value) for frames 150 on. Figure 12 shows the frame-by-frame normalized
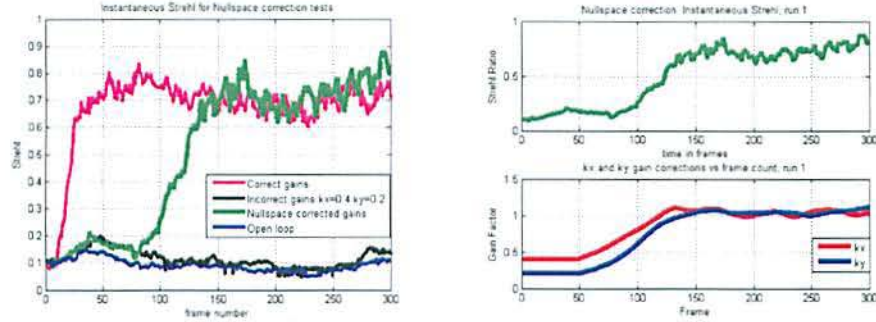

Fig. 11. *Instantaneous Strehl for $r_0 = 8.87$ cm, $Ry = 0.01$, $f_G = 24.0$ Hz. Nullspace corrected data (blue) vs uncorrected data (black). Right: Nullspace corrected instantaneous Strehl (top), frame-by-frame gradient gain factors kx and ky (bottom).*

power data for the same atmospheric conditions as were used in Figure 11, with the difference that the power in a 3x3 bucket was normalized by that of the closed loop correct gains case. By doing so, performance improvements due to the Nullspace algorithm were isolated from other changes that might have occurred in the system. Note that the pink curve is now always at 1, since it is normalized by itself at each frame. The blue and green curves are two identical Nullspace runs, which start out at the bottom, and end up fluctuating around the best closed loop AO performance. There was virtually no difference between the two Nullspace runs; they were taken in order to verify the repeatability of the algorithm.
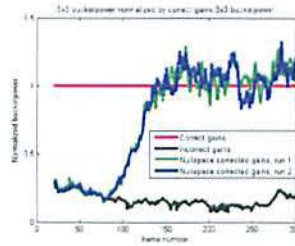

Fig. 12. *Data normalized by the correct gains closed loop AO. The two Nullspace runs are identical, showing the repeatability of the algorithm performance.*

Figure 13 shows several more Strehl plots that illustrate how well the algorithm worked for the different atmospheres presented in Table 2. Note that for the data shown in the upper left corner in Figure 13, we used a different set of field lenses compared to all other data sets. This could explain the fact that this data set has more stable plots and higher mean Strehl. For data shown in the lower left corner of Figure 13, Strehl ratio is varying highly for both correct and incorrect gains. This is due to the fact that our system was not fast enough to correct for high Greenwood frequencies. The important point is that the uncorrected extended gains plot is way below the correct gains one (the black curve is way below the pink curve), and the Nullspace corrected plot lines up very well with the regular closed loop AO one. For lower right plot in Figure 13, the Greenwood frequency was set even higher, at 82.6 Hz (based on 1 kHz system speed)., however the control filter gain was adjusted so that the system could keep up with the turbulence better. This explains better closed loop AO performance (pink curve) compared to lower left plot data, where f_G was 52.9 Hz, but the control gain was unadjusted. The important point is that the Nullspace performance is consistently good for both data sets, bringing the Strehl back to the regular AO performance level in each case.
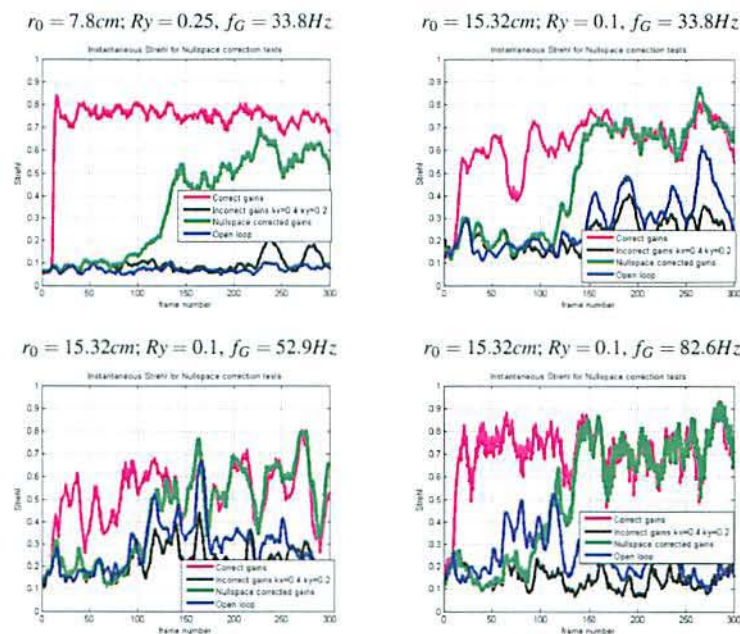

Fig. 13. *Strehl Ratio plots for several atmospheric sets. Note the Nullspace corrected data (green) climbs up to the closed loop AO case.*

7. Conclusion

We demonstrated that real time WFS gain correction technique based on null space of the reconstructor works well to improve the closed loop AO performance in various turbulence regimes. The technique is relatively insensitive to atmospheric conditions: for low to moderate turbulence, the Nullspace algorithm brings the system performance all the way up to the best possible closed loop AO performance; for more severe turbulence cases, the Nullspace technique does not go quite all the way to perfect closed loop AO level, but exhibits very significant increase in Strehl compared to data uncorrected for extended beacon gain changes. The algorithm produced stable, repeatable data with consistently improved Strehl. In the future we plan to incorporate a new optical source in the ASALT laboratory that would simulate a real extended beacon under different zenith angles. This will allow changing gains in the optical domain, as opposed to doing this in software as was done for the experiment described in this paper. In addition, the Nullspace technique needs to be combined with the algorithm that will vary gains from sub-aperture to sub-aperture based on the zenith angle and elevation. This will allow for yet a better method of compensation for extended nature of the sodium beacon.

8. Acknowledgements

References and links

[1] F. Roddier. *Adaptive Optics in Astronomy*. Cambridge University Press, Cambridge, UK, 1 edition, 1999.

[2] N. Moussaoui, B. R. Clemesha, and R. Holzlohner. Statistics of the sodium layer parameters at low geographic latitude and its impact on adaptive-optics sodium laser guide star characteristics. *Astronomy and Astrophysics*, 511(A31):1–8, 2010.

[3] K. P. Vitayaudom, D. J. Sanchez, D. W. Oesch, P. R. Kelly, C. M. Tewksbury-Christle, and J. C. Smith. Experimental analysis of perspective elongation effects using a laser guide star in an adaptive-optics system . SPIE, 2009.

[4] K. P. Vitayaudom, R. A. Vincent, J. D. Schmidt, and D. J. Sanchez. Analysis of Non-Uniform Gain for Control of a Deformable Mirror in an Adaptive-Optics System. In Richard Carerras, Troy Rhoadharmer, and John Gonglewski, editors, *2008 SPIE Annual Conference*. SPIE, 2008.

[5] E. Viard, F. Delplanckea, N. Hubin, and N. Ageorges. LGS Na-spot elongation and Rayleigh scattering effects on Shack-Hartmann wavefront sensor performances. In *Adaptive Optics Systems and Technology*, 1999.

[6] J. Véran and G. Herriot. Centroid gain compensation in shack-hartmann adaptive optics systems with natural or laser guide star. *J. Opt. Soc. Am. A*, 17(8):1430–1439, 2000.

[7] R. Conan, O. Lardiere, G. Herriot, C. Bradley, and K. Jackson. Experimental assessment of the matched filter for laser guide star wavefront sensing. *Appl. Opt.*, 48(6):1198–1211, 2009.

[8] L. Gilles and B. Ellerbroek. Shack-hartmann wavefront sensing with elongated sodium laser beacons: centroiding versus matched filtering. *Appl. Opt.*, 45(25):6568–6576, 2006.

[9] J. M. Beckers, M. Owner-Peterson, and T. Andersen. Rapid refocusing system for the euro50 telescope aimed at removing the perspective elongation of laser beacons. volume 5169. SPIE, 2003.

[10] C. Baranec, B. J. Bauman, and M. Lloyd-Hart. Concept for a laser guide beacon shack-hartmann wave-front sensor with dynamically steered subapertures. *Opt. Lett.*, 30(7):693–695, 2005.

DISTRIBUTION LIST

DTIC/OCP
8725 John J. Kingman Rd, Suite 0944
Ft Belvoir, VA 22060-6218   1   cy

AFRL/RVIL
Kirtland AFB, NM 87117-5776   2 cy

Patrick Kelly
Official Record Copy
AFRL/RDSAE   1 cy